

WIDEBAND NEGATIVE PERMITTIVITY METAMATERIAL FOR SIZE REDUCTION OF STOPBAND FILTER IN ANTENNA APPLICATIONS

M. A. Abdalla*, M. A. Fouad, H. A. Elregeily, and A. A. Mitkees

Department of Electronic Engineering, MTC University, Cairo, Egypt

Abstract—The design and simplified analysis of a compact and wide band (16%) negative permittivity complementary split ring resonator metamaterial is introduced. The proposed metamaterial component was applied to reduce the size of the feeding line filter of microstrip patch antenna for the sake of higher order harmonic suppression. The reduction has been done using only one element of complementary split ring resonator, while maintaining the antenna's performance. Simplified theoretical study and design of the proposed circuits has been presented. Moreover, experimental results have been done for validation and conformation purpose. Results confirm that almost 95% of the antenna noise harmonics power has been removed.

1. INTRODUCTION

One interesting goal in microwave circuits/antenna designs is the filtering of frequency bands for the purpose of undesired harmonic suppression and enhancement of microwave component performance. Many traditional approaches have been utilized for this purpose such as cascaded rejection band filters. However, wide bandwidth and size reduction are two main requirements that we should achieve while satisfying the previous goal. Size reduction objective can be fulfilled by making use of the ground area in microstrip configuration, by etching holes in the ground. An example for this is the use of electromagnetic band gap structures (EBG) [1, 2]. Although such techniques introduce wide band and decrease microwave circuit size, but they still need large area in the transverse plane, especially at lower frequencies.

Received 25 August 2011, Accepted 19 October 2011, Scheduled 31 October 2011

* Corresponding author: Mahmoud Abdelrahman Abdalla (maaabdalla@ieee.org).

Another solution for size reduction has been proposed using metamaterial (MTM) structures. Metamaterials can be defined as effective homogenous electromagnetic structures with unusual properties that do not exist in nature. Effective homogeneous electromagnetic structure can be constructed using electromagnetic ordered array scatters satisfying a sufficient long wavelength condition at RF/microwave frequencies to demonstrate particular electromagnetic properties [3]. These material concepts include artificial dielectric materials and magnetic materials which can exhibit positive or negative permittivity or permeability properties, respectively [3]. Studies confirm that the propagation of electromagnetic waves in metamaterial structures will have different characteristics, and accordingly, they have been employed in different RF/microwave either guided wave or radiated wave applications.

A medium with negative permeability or permittivity has an imaginary propagation constant such that the waves through it are evanescent waves. Therefore, it is a good candidate for satisfying the aforementioned purpose: filtering of frequency bands. In nature, plasma is a medium observed to have a negative permittivity below certain frequency called the plasma frequency. In 1996, Pendry et al. [4, 5] introduced artificial electrical plasma consisting of three dimensional array of intersecting thin straight wires whose electrical plasma frequency is dependent on the wire radius and spacing, and hence it is possible to design it in the microwave band [4]. However, such a 3D structure is not compatible with planar microwave applications.

In 2003, a new metamaterial negative permittivity planar structure based on the use of complementary split ring resonators (CSRRs) has been suggested [6]. CSRR is the dual of split ring resonator (SRR) which can demonstrate effective negative permeability. CSRR is implemented by etching them on the ground plane of microstrip strips. Since CSRRs are metamaterial structure, they oppose the sub wavelength criterion of metamaterials, i.e., CSRRs dimensions are much smaller than the guided wavelength. Hence, by using CSRRs, we can achieve high level of circuit miniaturization. Therefore, CSRRs have been utilized in different microwave and antenna applications [7–13].

However, one of the main goals in designing CSRRs is increasing their negative permittivity bandwidth. For achieving wideband negative permittivity, one solution is to use more than one etched CSRR unit cell with different dimensions [11]. Another solution is to use more unit cells of etched CSRRs with different orientation and dimensions [12, 13]. But, unfortunately, all these trials will result in

increasing the circuit size.

In this paper, we introduce a wide band negative permittivity stopband filter structure making use of CSRRs. The proposed CSRR filter has been applied to achieve size reduction of a microstrip stopband filter. For the sake of completeness, this compact CSRR stopband filter has been cascaded to a microstrip antenna used for the removal of undesired antenna higher harmonics. The compactness was achieved by the use of only one CSRR unit cell.

2. CSRR CONCEPT

It has been suggested that the use of periodic array of split ring resonator excited by a magnetic field parallel to ring axis is able to introduce an artificial negative permeability metamaterial that may be implemented as a three dimensional periodic structure [14]. However, the H-field excitation provided by the incident field on conventional split ring resonator is not strong enough to produce a noticeable effect. Thus, a multilayered architecture is required to produce a sufficient response. Therefore, in summary, we can say that use of SRR is not convenient with microstrip configuration.

On the other hand, complementary split spring resonator, excited by an electric field polarized in the axial direction of the ring so that it results in negative permittivity, was introduced to overcome this problem [6]. From electromagnetic theory, if the thickness of the metal plates is zero, and the conductivity that it exhibits is infinite, then the apertures behave as perfect magnetic conductors, and hence the CSRR behaviour can be considered as a dual (or complementary) of SRR. Therefore, CSRR can be easily fabricated using microstrip configuration by etching the rings in the ground plane beneath the upper microstrip transmission strip.

From the circuit point of view, the CSRR particle can be described as a parallel resonant tank with inductance L_c and capacitance C_c and behaves as an electric dipole which is excited by an external axial electric field (in this case the electric field of the microstrip line). L and C represent the per unit length inductance and capacitance of the host line which is electrically coupled to the CSRR. The lumped element equivalent circuit model for the CSRR loaded transmission line is depicted in Figure 1. The negative permittivity of the CSRR is centered at the resonant tank circuit whose resonant frequency (f_0) can be described by

$$f_0 = \frac{1}{2\pi\sqrt{L_c C_c}} \quad (1)$$

3. STRUCTURE

Conventional microstrip antennas in general have attractive features of low profile, lightweight, easy fabrication, and conformability to mounting hosts. However, they have a major drawback of higher order harmonic radiation which may interfere with outside band users. Such a problem can be overcome by cascading the microstrip antenna to a filter circuit, and stepped impedance resonator filter is one popular way [15]. This technique may result in extra antenna size. A recent solution is to make use of the CSRR filtering properties and etch them on the ground of the antenna feeding line [11]. However, the use of multiple cells may need long feeding line, and hence this may also increase the overall antenna size. In this section, we introduce the use of only one CSRR unit cell for the sake of higher harmonic suppression.

The concept of optimization use of a CSRR unit cell was applied to a conventional rectangular patch antenna. The rectangular patch antenna was matched to a $50\ \Omega$ feeding microstrip transmission line section. A circular shaped CSRR unit cell was etched on the ground beneath the feeding microstrip transmission line. The used substrate is Rogers RT\duroid 5880 substrate with relative permittivity $\epsilon_r = 2.2$ and 0.787 mm thickness. The CSRR particle dimensions are $r = 2.6\text{ mm}$, $c = 0.4\text{ mm}$, $d = 0.3\text{ mm}$, and $g = 0.1\text{ mm}$. The detailed antenna geometry is shown in Figure 2(a) where $W = 63.8\text{ mm}$, $L = 53.8\text{ mm}$, $L_c = 30\text{ mm}$, $L_f = 18.6\text{ mm}$ and $W_f = 2.4\text{ mm}$.

The fabricated antenna is shown in Figures 2(b) and (c). The circuit pattern fabrication process was carried out by using wet etching of the metallization to remove the unwanted parts of the metallization and form the circuit patterns required. First, a photoresist protecting

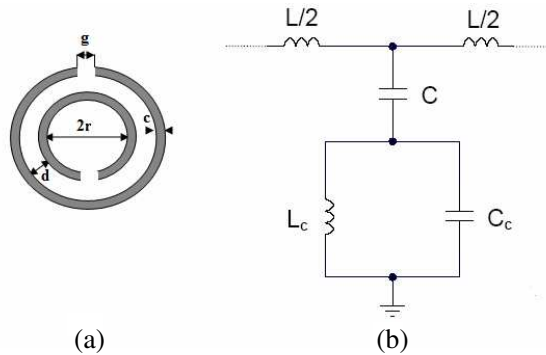


Figure 1. (a) The CSRR particle geometry. (b) The equivalent circuit model for the basic cell CSRR loaded microstrip line.

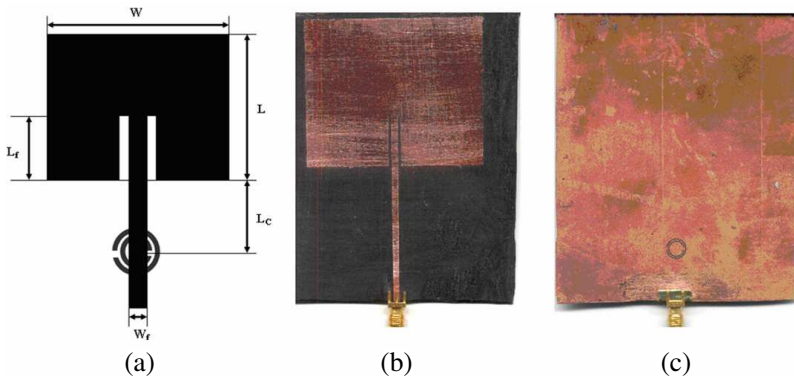


Figure 2. (a) Microstrip antenna loaded with CSR feeding transmission line layout. (b) The fabricated microstrip patch antenna loaded with CSR (upper layer). (c) Lower fabricated layer.

the layer patterns was deposited on the conductor layer face and patterned using the lithography process. Second, the unwanted parts of the metallization were removed by wet etching using the etching solution ($\text{NH}_4\text{OH} : \text{H}_2\text{O}_2 : \text{H}_2\text{O} = 1 : 1 : 4$). Finally, the photoresist was dissolved by acetone.

4. DESIGN

The design objective for the antenna harmonic suppression was based on cascading the antenna to a stopband filter within the antenna harmonics frequencies. For the sake of antenna miniaturization, the stopband filter was designed to be within the same antenna feeding transmission line. This can be done by using a CSR etched on the ground plane of the feeding microstrip transmission line. Such a filter is a negative permittivity metamaterial one whose negative permittivity frequency band achieves the desired stopband, i.e., the frequency band to be suppressed of the antenna harmonics. This frequency band was obtained by a proper CSR dimension choice which results in resonant frequency as calculated from (1). This design was done as in the following steps using the electromagnetic full wave simulation employing a commercial finite element software ANSOFT-HFSS.

First, a conventional rectangular patch antenna, without using CSR, was designed at 1.8 GHz to radiate efficiently and exhibit 50Ω input impedance [16]. The patch antenna was excited by a 50Ω microstrip transmission line which is inset feed to the antenna a distance L_f as shown in Figure 2(a) for matching purpose [16]. The

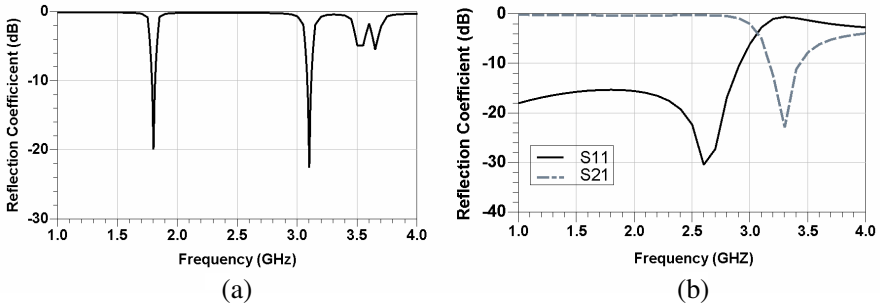


Figure 3. (a) The reflection coefficient of a conventional microstrip antenna (without CSRR) and (b) the scattering parameter magnitudes of the feeding transmission line loaded with CSRR.

simulated antenna return loss is shown in Figure 3(a). As shown, the microstrip patch antenna can radiate at 1.8 GHz with a return loss 20 dB. However, at 3.1 GHz, it has spurious higher order harmonic that result in return loss greater than 22 dB in addition to some additional spurious radiations present around 3.5 GHz.

For suppressing the aforementioned harmonics, the CSRR negative permittivity stop band was designed to cover frequencies including the above frequencies 3.1 GHz. For compactness purpose, only one CSRR was desired which was achieved in the design by the proper design of the unit cell CSRR. This can be explained by simulating the feeding transmission line loaded with CSRR unit as a two port network using HFSS. On simulation, we have assumed $50\ \Omega$ feeding SMA connector at one end and $50\ \Omega$ patch antenna at the other end. After a round of optimization process for the previously analytically investigated CSRR, the proposed CSRR unit cell was designed. The full wave simulated scattering parameters for this negative permittivity metamaterial feeding transmission line is shown in Figure 3(b). As shown, the results confirm that the CSRR has a stopband in frequency band 3 GHz–3.5 GHz which predicts its possibility to suppress harmonics shown in Figure 3(a).

The design of the CSRR has been fulfilled by investigating the performance of the equivalent circuit model, illustrated in Figure 1(b), for the employed CSRR. Next, the design was validated by comparing the circuit model results with the same results obtained from HFSS, which are illustrated in Figure 3(b). From this comparison, we have find that the CSRR equivalent capacitance (C_c) and inductance (L_c), shown in Figure 1(a), are 3.5 pF and 0.6 nH, respectively. Substituting these values in (1), we find that CSRR demonstrates resonant frequency at approximately 3.45 GHz. This frequency is

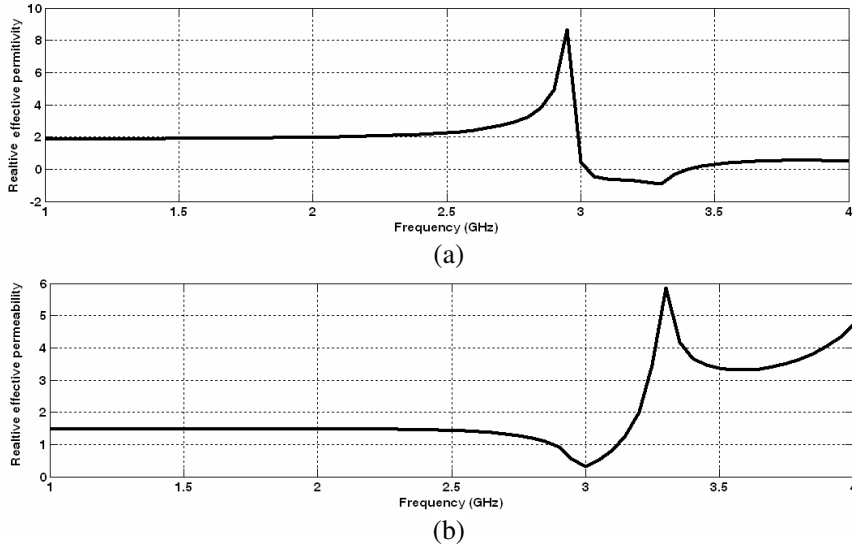


Figure 4. The effective permittivity and permeability of the microstrip feeding transmission line loaded with the CSRR.

approximately the same resonant frequency which can be observed in Figure 3(b).

The negative permittivity can be confirmed by extracting the effective constitutive parameters, i.e., the electric and magnetic permeabilities, of the microstrip feeding transmission line loaded by the CSRR using the simulated scattering parameters shown in Figure 3(b) [17]. The results are illustrated in Figure 4. It is obvious that the metamaterial transmission line demonstrates positive effective permeability with negative effective permittivity within the frequency band approximately from 3–3.5 GHz approximately, a fractional bandwidth of 16%, which also agrees with the stopband in Figure 3(b).

In Figure 2(a), one can find the maximum CSRR element dimension ($2r + 2c + d = 6.3$ mm). Also, the guided wavelength (λ_g) can be calculated to be $\lambda_g = 73$ and 63 mm at lower and upper frequencies of frequency band characterized by negative permittivity shown in Figure 4(a), i.e., from frequency = 3 GHz to 3.5 GHz. Thus, we can confirm that the maximum CSRR particle dimension is at maximum = $\lambda_g/10$ which agrees with the standard condition for subwavelength structure of metamaterial [3]. This conclusion confirms the effective negative permittivity required to describe the employed CSRR structure as a metamaterial one.

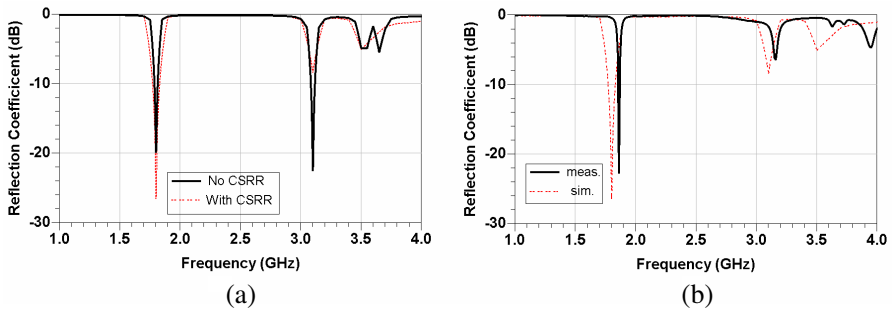


Figure 5. (a) The simulated reflection coefficient of the microstrip antenna with and without the use of CSRR. (b) A comparison between measured results and simulated results employing CSRR filter.

5. RESULTS AND DISCUSSION

The two previous individual circuits, the patch antenna and its negative permittivity feeding line, were cascaded and simulated together. The simulated return loss of the proposed antenna is shown in Figure 5(a). The figure also illustrates the simulated reflection coefficient of the microstrip patch antenna for comparison purpose.

As shown in the figure, the results confirm that the antenna can still radiate effectively at 1.8 GHz with an improved return loss that is better than 25 dB. On the other hand, the harmonic exists at 3.1 GHz of the conventional patch antenna was suppressed by using the CSRR from approximately 22 dB to 8 dB which represents approximately 66% harmonic level reduction. Moreover, a little bit enhancement in the other small harmonics around 3.5 GHz was noticed. Over the whole frequency band, no other harmonics were added to the antenna performance. Therefore, we can claim that the antenna cannot radiate at these frequencies, hence it confirms the harmonics suppression.

From previous discussions, we can claim that the removal of the spurious harmonic at 3.1 GHz requires to load the feeding transmission line with only one unit cell with maximum dimensions = 6.3 mm which is equivalent to $0.09\lambda_g$ ($\lambda_g = 70.4$ mm at 3.1 GHz). Up to our knowledge, no stopband filter can be realized using such a small length. For comparison purpose, the harmonic suppression goal in [11] was fulfilled using two CSRR elements whose overall length is $0.27\lambda_g$.

To verify the theoretical study and simulation results discussed in previous sections, the metamaterial antenna was fabricated, and the return loss of the antenna was measured using Hewlett Packard 8510C VNA System through a 50 Ω SMA connector. A comparison between the simulated and measured results is shown in Figure 5(b). The

comparison demonstrates reasonable agreement between the measured and simulated results, and there is approximately no more than 100 MHz frequency shift between the measured and simulated results. It obvious that both results confirm the suppression of the higher order harmonics by more than 15 dB compared to original patch antenna.

Moreover, the antenna performance has been reconsidered by examining the radiation pattern of the antenna to ensure that the employed CSRR did not affect the antenna properties. The simulated 3D radiation pattern at 1.8 GHz is shown in Figure 6. It is clear that the metamaterial antenna preserves the omnidirectional pattern of conventional antenna. This can be made clearer by illustrating the normalized 2D radiation pattern in the three basic planes as shown in

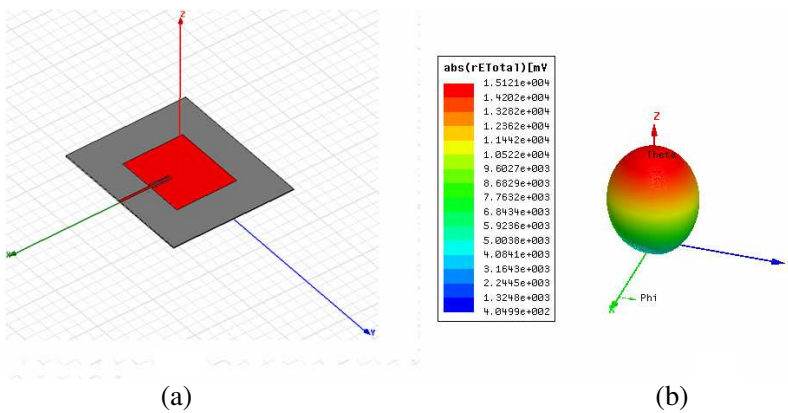


Figure 6. (a) The antenna cascaded with the CSRR filter geometry. (b) The 3-D radiation pattern of the antenna cascaded with the CSRR filter at 1.8 GHz.

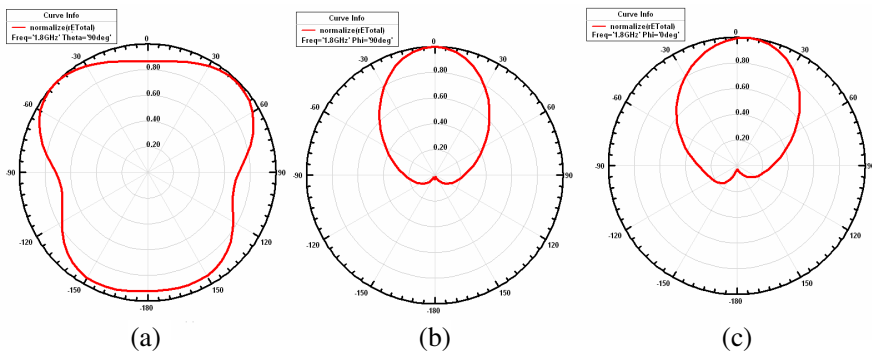


Figure 7. The 2D radiation pattern of the antenna cascaded with the CSRR filter.

Figure 7. As seen, the plane is almost isotropic in the horizontal plane (XY plane, $\theta = 90$), and its maximum in either XZ or YZ plane is along the Z axis ($\theta = 0$).

In addition, the antenna polarization was checked by comparing the co- and cross-polarized gains in both E plane (XZ) and H plane (YZ) as plotted in Figure 8. It is obvious that the difference between the two gains is almost greater than 40 dB in both E/H planes.

Further check of the harmonic suppression was verified by studying the 3D radiation pattern at the spurious frequency (3.1 GHz) which is illustrated in Figure 9. By comparing this 3-D radiation pattern to that at 1.8 GHz in Figure 6(b), it is quite clear that the antenna has a main pattern at 1.8 GHz with the maximum radiation along Z axis

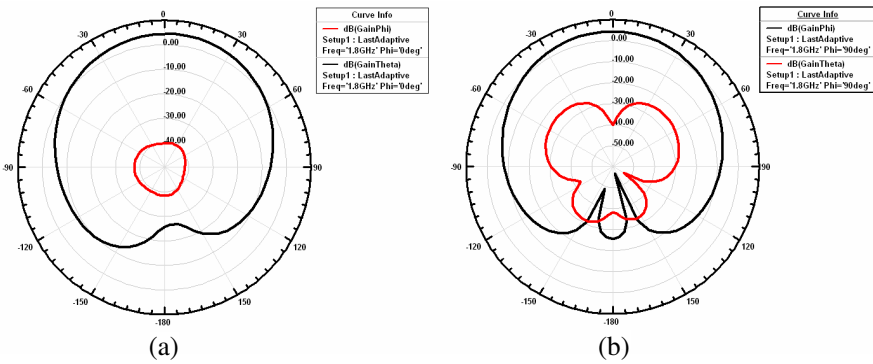


Figure 8. Comparison between the co-polarized and cross-polarized gain in H/E planes of the antenna cascaded with the CSRR filter.

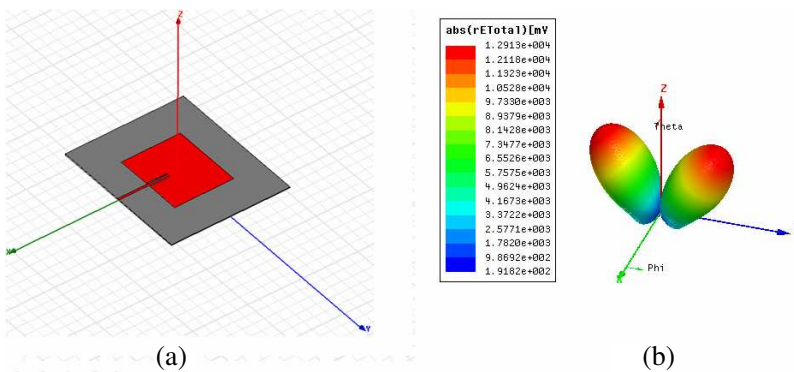


Figure 9. (a) The antenna cascaded with the CSRR filter geometry. (b) The 3-D radiation pattern of the antenna cascaded with the CSRR filter at 3.1 GHz.

whereas in the second case at 3.1 GHz, the radiation pattern consists of two smaller lobes with almost zero radiation along the Z axis. In other words, we can claim that the antenna no longer radiates along the Z axis at the spurious frequency, at 3.1 GHz, which confirms the spurious harmonic suppression.

6. CONCLUSION

A wide band negative permittivity metamaterial CSRR was introduced. The proposed CSRR was designed to introduce a compact microstrip filter implemented using only one unit cell CSRR. The designed filter was cascaded with a microstrip patch antenna for higher order harmonics removal. The design was introduced and validated using electromagnetic full wave simulation, and confirmed using measurements. Results confirmed that a compact CSRR microstrip filter (only $0.09\lambda_g$ at suppressed harmonic frequency) of wideband negative permittivity bandwidth (16%) can suppress up to 95% of higher order harmonics without changing the properties of the patch antenna.

REFERENCES

1. Radisic, V., Y. Qian, R. Coccioli, and T. Itoh, "Novel 2-D photonic, bandgap structure for microstrip lines," *IEEE Microwave Guided Wave Lett.*, Vol. 8, 69–71, Feb. 1998.
2. Yang, F. R., K. P. Ma, Y. Qian, and T. Itoh, "A uniplanar compact photonic-bandgap (UC-PBG) structure and its applications for microwave circuits," *IEEE Trans. Microwave Theory Tech.*, Vol. 47, 1509–1514, Aug. 1999.
3. Caloz, C. and T. Itoh, *Electromagnetic Metamaterials: Transmission Line Theory and Microwave Applications*, John Wiley & Sons, Inc., 2006.
4. Pendry, J. B., A. J. Holden, D. J. Robbins, and W. J. Stewart, "Low frequency plasmons in thin-wire structures," *Journal of Physics: Condensed Matter*, Vol. 10, 4785–4809, 1998.
5. Pendry, J. B., A. J. Holden, W. J. Stewart, and I. Youngs, "Extremely low frequency plasmons in metallic mesostructures," *Physical Review Letters*, Vol. 76, 4773–4776, 1996.
6. Falcone, F., T. Lopetegi, J. D. Baena, R. Marques, F. Martin, and M. Sorolla, "Effective negative-epsilon stopband microstrip lines based on complementary split ring resonators," *IEEE Microwave and Wireless Components Letters*, Vol. 14, 280–282, 2004.

7. Qiang, L., Y.-J. Zhao, Q. Sun, W. Zhao, and B. Liu, "A compact UWB HMSIW bandpass filter based on complementary split-ring resonators," *Progress In Electromagnetics Research C*, Vol. 11, 237–243, 2009.
8. Lai, X., Q. Li, P.-Y. Qin, B. Wu, and C.-H. Liang, "A novel wideband bandpass filter based on complementary split-ring resonator," *Progress In Electromagnetics Research C*, Vol. 1, 177–184, 2008.
9. Al-Naib, I. A. I. and M. Koch, "Coplanar waveguides incorporating SRRs or CSRRs: A comprehensive study," *Progress In Electromagnetics Research B*, Vol. 23, 343–355, 2010.
10. Zhang, Q.-L., W.-Y. Yin, S. He, and L.-S. Wu, "Evanescent-mode substrate integrated waveguide (SIW) filters implemented with complementary split ring resonators," *Progress In Electromagnetics Research*, Vol. 111, 419–432, 2011.
11. Ali, A. and Z. Hu, "Microstrip patch antenna incorporating negative permittivity metamaterial for harmonic suppression," *The 2nd European Antenna and Propagation Conference EuCAP 2007*, 1–3, 2007.
12. Khan, S. N., X. Liu, L. Shao, and Y. Wang, "Complementary split ring resonators of large stop bandwidth," *Progress In Electromagnetics Research Letters*, Vol. 14, 127–132, 2010.
13. Ali, A. and Z. Hu, "Broadband antenna with frequency notch characteristic based on complementary split-ring resonators," *Antennas and Propagation Society International Symposium*, 3468–3471, 2007.
14. Pendry, J. B., A. J. Holden, D. J. Robbins, and W. J. Stewart, "Magnetism from conductors and enhanced nonlinear phenomena," *IEEE Trans. Microwave Theory Tech.*, Vol. 47, 2075–2084, Nov. 1999.
15. Vendik, I. B., D. V. Kholodnyak, I. V. Kilmakova, E. V. Serbryakova, P. V. Kapitnova, F. Martin, J. Garcia, I. Gil, and M. Gil, "Applications of right/left handed and resonant left handed transmission lines for microwave circuit design," *The 36th European Microwave Conference Proceedings*, Manchester, UK, 2006.
16. Balanis, C. A., *Antenna Theory Analysis and Design*, 3rd edition, John Wiley & Sons, Inc., 2005.
17. Mao, S.-G., S.-L. Chen, and C.-W. Huang, "Effective electromagnetic parameters of novel distributed left-handed microstrip lines," *IEEE Trans. Microwave Theory Tech.*, Vol. 53, No. 4, 1515–1521, Apr. 2005.